1995-09

How Listing's Law May Emerge from Neural Control of Reactive Saccades

HOW LISTING'S LAW MAY EMERGE FROM NEURAL CONTROL OF REACTIVE SACCADES

Christopher A. Pribe and Daniel Bullock

September 1995

Technical Report CAS/CNS-95-027

Boston University Center for Adaptive Systems and
Department of Cognitive and Neural Systems
111 Cummington Street
Boston, MA 02215

How Listing's Law May Emerge from Neural Control of Reactive Saccades

Christopher A. Pribe [*] Daniel Bullock [†]

Center for Adaptive Systems and
Department of Cognitive and Neural Systems
Boston University, 111 Cummington Street, Boston, MA 02215

[*]Supported in part by DARPA (AFOSR 90-0083) and ONR (ONR N00014-92-J-1309).
[†]Supported in part by ONR (ONR N00014-92-J-1309) and ONR (ONR N00014-95-1-0409).

Abstract

We hypothesize that Listing's Law emerges as a result of two key properties of the saccadic sensory–motor system: 1) The visual sensory apparatus has a 2–D topology and 2) motor synergists are synchronized. The theory is tested by showing that eye attitudes that obey Listing's Law are achieved in a 3–D saccadic control system that translates visual eccentricity into synchronized motor commands via a 2–D spatial gradient. Simulations of this system demonstrate that attitudes assumed by the eye upon accurate foveation tend to obey Listing's Law.

1 Introduction

The origin of Listing's Law has remained a mystery since its discovery over a century ago. Listing's Law is a kinematic regularity that is exhibited by human saccadic eye movements without evident cause. After a short description of the Law, we present our theory that Listing's Law obedient behavior emerges when the needs of and constraints on saccadic learning and performance interact with the properties of geometric rotations.

Listing's Law is a kinematic regularity of human saccadic eye movements first observed by Listing and Helmholtz (Helmholtz, 1867/1962). It says that a unique *displacement plane* is associated with every gaze direction, g, and that any saccade beginning at g, regardless of direction or amplitude, will rotate the eye around an axis that lies in this plane. There is one and only one gaze direction whose displacement plane is orthogonal to it. This gaze direction is called the primary position and its displacement plane is called *Listing's Plane.* There is variability in the adherence of saccadic eye movements to Listing's Law (Ferman et al, 1987) and violations occur for some other eye movements. For example, humans violate Listing's Law during visual pursuit of non–point targets (Tweed and Vilis, 1992b). The location of the primary position can vary between individuals in monkeys and humans (Tweed and Vilis, 1990c). The location of the displacement plane may vary with vergence (Tweed and Vilis, 1992a).

We theorize that topological restrictions on the visual sensory apparatus used for the purpose of learning saccadic control and the consistent synchronization of the motor synergists that move the eye lead to the emergence of Listing's law. That the visual sensory apparatus has fewer dimensions than the oculomotor plant has rotational degrees of freedom requires *that* there be a projection from the 3–D manifold of eye movements into a reduced, 2–D representation. That there is a consistent synchronization of the motor synergists that control eye movements (Scudder, 1988) specifies *which* projection will result. Our theory implies that Listing's Law is not imposed on a saccadic control system capable of 3–D control. Rather it is a consequence of the processes and mechanisms whereby control over a 3–D plant is eventually achieved. The Law is the result of a control system with limited sensory resources capitalizing on a geometric artifact that results from the performance of the plant it is trying to control. In particular, it is the need to map 2–D retinotopic sensory representation onto a set of motor commands capable of controlling a non–commutative 3–D plant that leads to the emergence of Law abiding ocular behavior. We propose that the synchronization of synergists realized by the coupled, parallel design of the saccadic control system (Scudder, 1988) is also critical for the emergence of Listing's Law. In particular, synchronization implies a preferential sampling of possible rotations. That is, whereas the horizontal and vertical saccadic commands of the naive controller underspecify the behavior of the non–commutative plant, synchronization completes the specification by inducing the plant to compose the rotations in an invariant way.

Rotational operations are not in general commutative: Rotation A followed by rotation B does not yield the same result as rotation B followed by rotation A. However, a hint

about how nature might get sufficiently consistent behavior from a non–commutative 3–D plant using commands that originate from a 2–D retinotopic representation comes from the observation that infinitesimal rotations are commutative. This is shown formally in the Appendix. Informally, it is easy to see that accumulating rotations starting with a small fraction of A, followed by a small fraction of B, followed by a small fraction A and so on, until both rotations are complete, is little different from accumulating a set of rotations in a similar sequence which however begins with a small fraction of B. Since muscles act in concert, that is, there is a synchronization of synergists, it is necessary to use a formalization, such as that used here, that allows simultaneous rotations. Note that it is not the case that arbitrary saccadic rotations comprised of cumulative, commutative infinitesimal rotations are themselves commutative. In a sense, though, truly simultaneous rotation implies that the 'most nearly commutative' rotation will result. Or stated another way, for saccades to random sequences of targets the effects of the non–commutativity of the oculomotor plant will be minimized. This may not be good enough for competent single–step saccadic control, but it is good enough to provide a stable baseline for learning. So long as the learning is sensitive to initial eye position, as well as to target position, this is good enough to bootstrap an adaptive system. It does not matter whether the learning occurs after failed saccades, as proposed by Grossberg and Kuperstein (1986), or after successful saccades as proposed by Pribe (1994).

In one recent model, Listing's Law has been included in a saccade generation system by the imposition of a 3–D Listing's Law operator (Tweed and Vilis, 1990a). Our approach highlights another theoretical possibility as described above: that Listing's Law, which is an initial–position–relative planar (2–D) constraint on rotations of a spatial (3–D) object, reflects a neural design that treats saccade generation as if it were a 2–D problem. In this design, saccadic gaze errors are measured in 2–D and the neural channels used to control the 6 extraocular muscles are constrained, by a preformed mapping, to behave like a 2 degree–of–freedom (DOF) system during saccades. When this system is allowed to make iterative saccades that result in accurate foveations, the resultant eye attitudes do, in fact, conform to Listing's Law.

2 Translating Visual Eccentricity into Motor Command Signals via a Spatial Gradient

When a light that has fallen on the retina is to be foveated, how does the retinotopic location of the light calibrate the saccade? In their solution to this question Grossberg and Kuperstein (1986) introduce two mechanisms to transform visual eccentricity into a specification of muscle length change. These mechanisms are: 1) a preferential assignment of the retinotopic target location to the extraocular muscle pairs via a *sector map* and 2) a *spatial gradient* of connection strength that is a function of target light eccentricity.

The purpose of the two mechanisms is to generate motor signals that will rotate the

eye approximately the correct direction and distance to foveate the target. Even given the ability to send the eye in the correct general direction by about the right amount, adaptive modifications would be needed to fine–tune saccade accuracy. Grossberg and Kuperstein (1986) describe mechanisms for improving saccade accuracy based on reducing the residual visual error after each saccade attempt. Pribe (1994) has taken an alternative approach. In this approach, motor learning is gated by foveation in order to improve saccade accuracy. That is, saccade accuracy is improved by 'turning on' motor learning only when the target is foveated.

The sector map is a directional mechanism whereby the orientation of the target light on the retina may be used to create and allocate a motor command signal to the various muscle pairs. The spatial gradient specifies that target lights that are more eccentric on the retina will result in a larger change in muscle lengths. For example, if a target light were horizontally displaced from the fovea, the sector map and spatial gradient would cooperate to alter the lengths of the lateral and medial recti (LMR), rather than altering the lengths of the superior and inferior recti (SIR) and the superior and inferior obliques (SIO), because only the LMR can horizontally redirect the fovea to cover the target. In Grossberg and Kuperstein (1986) the surface of the retina was mapped by three pairs of opposing hemifields. The muscles of each agonist–antagonist pair were then assigned to each hemifield pair. When a target light fell in one hemifield, resultant commands caused the length of one muscle, say the agonist, to increase while its antagonist's length decreased. A light falling in the opposite hemifield had the opposite effect. Taken together all of the hemifields in their various orientations are called a sector map. The output of the sector map is filtered through the spatial gradient so that the final signal provides a prewired or unconditioned estimate of the correct distance and direction for a saccade to a target falling in one or another initial sector.

The sector map used here differs from that described by Grossberg and Kuperstein (1986) in the number and orientation of the hemifield pairs and spatial gradients. The sector map of Figure 0.1 was designed to reflect the hypothesis that the neural representation is reduced by one dimension relative to the underlying geometry of the muscles and their actions in 3 dimensions, as shown in Figure 0.2. Thus only two hemifield pairs and spatial gradients are used, though there are three oculomotor muscle pairs. A functional reason for this is as follows. While it is appropriate to assign the horizontal dimension of the retinal surface to the lateral and medial recti, it is not appropriate to assign retinotopically opposed hemifields to either the SIR or the SIO muscle pairs by themselves. Inspection of Figure 0.2 shows that neither the actions of the SIO nor those of the SIR are exactly opposed with respect to the resultant motion of targets on the retina. However, the co–action of two imperfectly opposed pairs may result in a more perfect opposition, as can be seen by examination of the oculomotor muscle action shown in Figure 0.2. This suggests that, for purposes of saccadic control, the muscles of the eye may be grouped in two sets: those which move the eye primarily in the horizontal direction, the lateral and medial recti, and those whose synergetic action can move the eye primarily in the vertical direction, namely the superior and inferior recti *and* the superior and inferior obliques. The resulting sector map design is

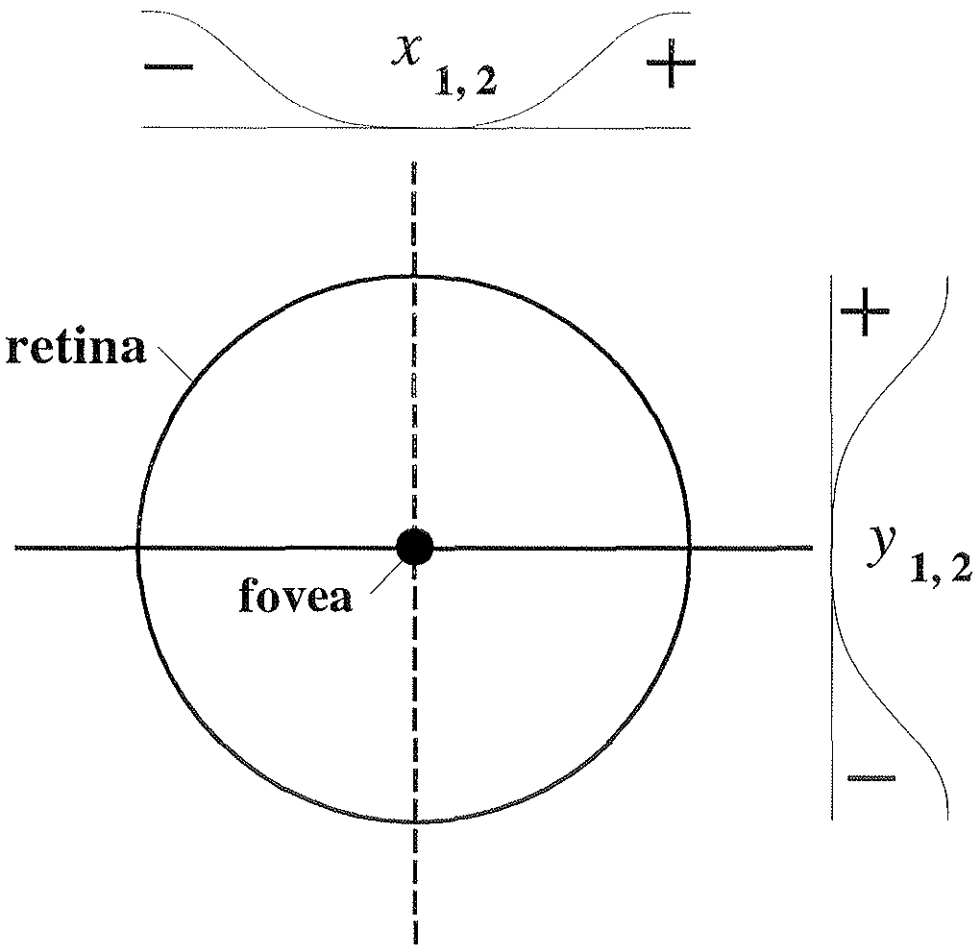

Figure 1: The sector map: Two hemifield pairs and spatial gradients capture the position of targets on the retina in two orthogonal dimensions, x and y. The output of the sector map in the x dimension corresponds to the lateral and medial recti. The y dimension output corresponds both to the superior and inferior obliques and to the superior and inferior recti. There is no bias between the muscle pairs. The position of the first light, (x_1, y_1), is passed through a gradient and provides a rough estimate of the correct distance and direction of the saccade. The position of the first light, (x_1, y_1) is also passed as part of the input vector to the adaptive gain stage. The position of the second light, (x_2, y_2), provides an error signal for the accuracy of the saccade. If the target has not been foveated, the second light signal may be used as a first light signal for a corrective saccade. A linear spatial gradient is used for the simulations shown in this article.

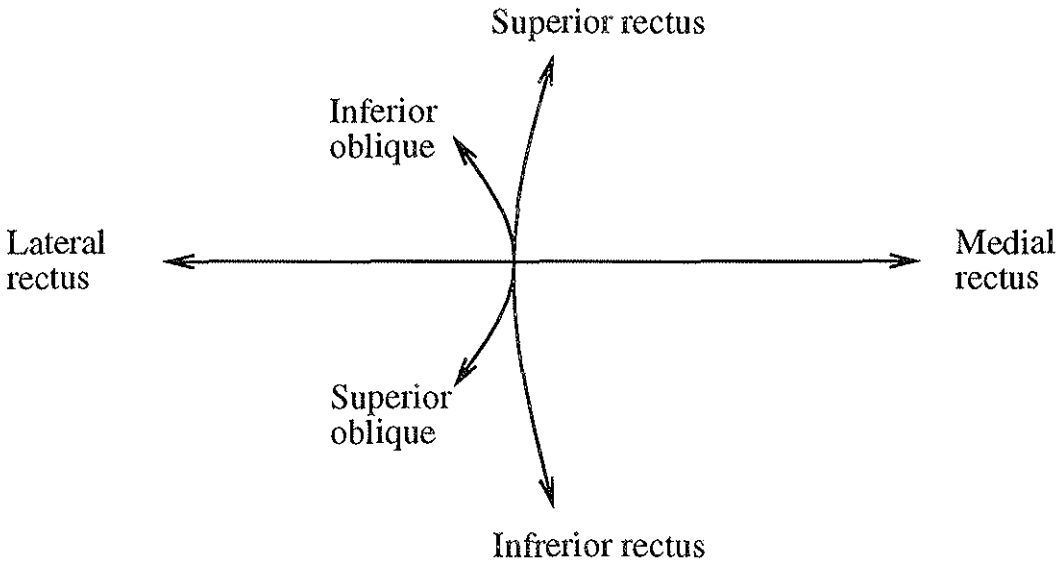

Figure 2: The movement directions of the right eye resulting from the individual actions of the eye muscles (after Gouras, in Kandel and Schwartz, 1985).

one in which the hemifield pairs are orthogonal and reflective of the two dimensional topology of both the retina and important saccadic control sites, such as the superior colliculus (Hepp *et al*, 1993).

3 Neural Control of Naive Reactive Saccades

Even if such a neural simplification exists, the actual motion of the eye will be 3–D trajectories. A non–adaptive neural network/oculomotor model architecture for reactive saccades in 3–D space is shown in Figure 0.3. Beginning from the retina in the upper right hand corner of the figure, a saccade is performed in the following steps: A transform from spatial to retinotopic coordinates is performed, a transform from retinotopic to motor coordinates is performed, a simplified saccade generator specifies motor commands via the tonic cells, muscle lengths track tonic cell activities, and a saccade is performed. The initialization of the oculomotor plant and other details of the simulation are also described.

A transform from spatial to retinotopic coordinates is performed. The location of the target on the retina, (R, θ), is computed in retinotopic polar coordinates via spherical trigonometry from the gaze attitude and the target position in space, g and t respectively, as described in Pribe (1994). The fovea is considered to be the origin of the retinotopic frame. The polar coordinates of the target are converted to cartesian coordinates for representation in a retinotopic map that is dimensionally consistent with the sector map described above.

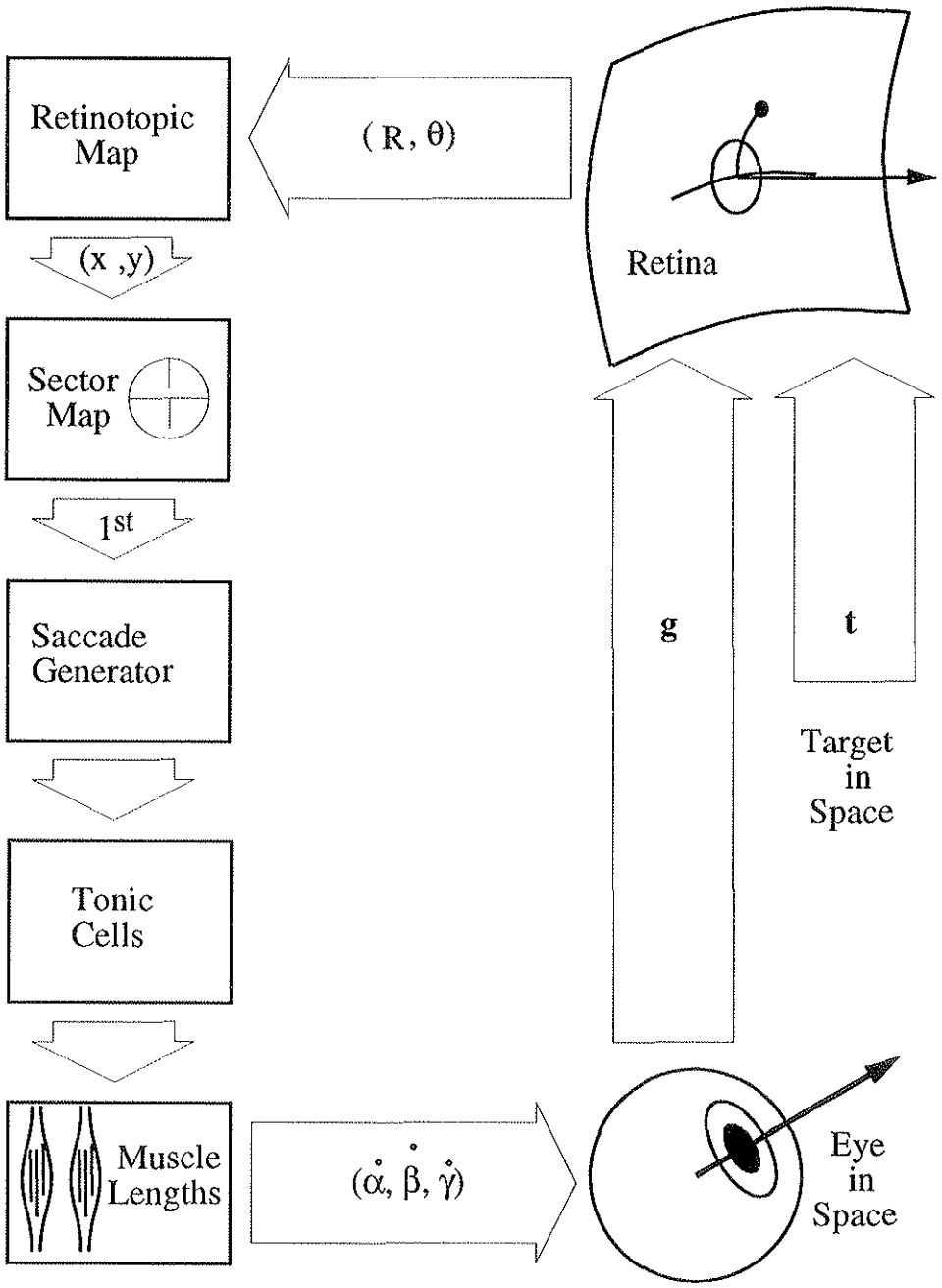

Figure 3: A neural network reactive saccadic control system that foveates targets through successive approximation. This neural network is capable of controlling the eye in space for both the pulley and the no-pulley models. Unless otherwise marked the coordinates of the information transferred from one module to the next is in muscle coordinates.

The target's retinotopic coordinates are

$$x = A * R\,cos(\theta) \tag{1}$$

and

$$y = A * R\,sin(\theta), \tag{2}$$

where x and y are the horizontal and vertical target eccentricities respectively, R and θ are the target coordinates in polar coordinates, and A is a scaling factor. The location of the first light[1] is denoted by (x_1, y_1) and the location of the second light is denoted by (x_2, y_2). Since the origin of this coordinate frame is the fovea, these values can be both positive and negative.

A transform from retinotopic to motor coordinates is performed. The sector map position of the first light, (x_1, y_1), both 1) represents the target coordinates and 2) provides a rough estimate of the correct distance and direction of the saccade because of the graded projection from the sector map to the motor channels. The pre–saccadic target or first light location on the retina, (x_1, y_1), is the source of unconditioned muscle signals via a spatially graded projection. The output of the sector map is so organized that the horizontal retinotopic dimension, x, is linked to the lateral and medial recti (LMR) and the vertical retinotopic dimension, y, is linked to both the superior and inferior recti (SIR) and to the superior and inferior obliques (SIO). There is no bias in the projection to these two 'vertical' muscle pairs. Throughout the simulations, opponent motor channels, e.g. agonist–antagonist muscle pairs, were represented as the positive and negative values of scalar quantities.

A simplified saccade generator specifies motor commands via the tonic cells. Saccades are, *in vivo*, generated via a pulse and a step in activity (Kandel and Schwartz, 1985). The pulse serves to overcome inertia. The step change in activity represents the motor coordinates of the new eye attitude. The saccade generator used in the simulations has been idealized to abstract away from irrelevant details. The pulse is not included, since the oculomotor model does not include inertia. The output of the saccade generator represents the step change by a discrete change in a tonic cell activity level.

The response to an activated target is computed in a single step, so that the new tonic cell activity level to control a saccade attempt, a, is

$$T_{LMR}(a) = T_{LMR}(a-1) + G_{lm}\,x_1, \tag{3}$$

$$T_{SIR}(a) = T_{SIR}(a-1) + G_{si}\,y_1, \tag{4}$$

$$T_{SIO}(a) = T_{SIO}(a-1) + G_{si}\,y_1, \tag{5}$$

[1]The terms *first light* and *second light* were coined by Grossberg and Kuperstein (1986) and refer to the presaccade and postsaccade retinotopic target locations respectively.

where $T(a)$ is the activity level specifying the tonic command for a given saccade attempt, G_{lm} is the spatial gradient gain to the lateral and medial recti, G_{si} is the spatial gradient gain to both of the superior and inferior muscle pairs, and x_1 and y_1 are the sector map eccentricities of the first light. The output of the sector map via the unconditioned pathway is a single quantity used to represent opponent muscle channels. Since this quantity may be positive or negative, the tonic cell activities are also positive or negative.

Muscle lengths track the tonic cell activities by

$$\dot{\alpha} = (T_{LMR} - \alpha)J \tag{6}$$

$$\dot{\beta} = (T_{SIR} - \beta)J \tag{7}$$

$$\dot{\gamma} = (T_{SIO} - \gamma)J \tag{8}$$

where α, β, and γ set the muscle length balance for the the lateral and medial recti (LMR), superior and inferior recti (SIR), and the superior and inferior obliques (SIO) muscle pairs respectively and J is the tracking rate. For all the simulations, $J = 1$. Tonic cell activities are assumed to reflect the balance of muscle lengths for the three agonist–antagonist oculomotor muscle pairs, so that $\dot{\alpha}$, $\dot{\beta}$, and $\dot{\gamma}$ are the rates of muscle length change used to rotate the eye in space.

A saccade is performed. Eye rotations are simulated using the following unified mathematical model of the oculomotor plant (Pribe and Cohen, 1995 and Pribe, 1994). The model has a number of features required for accurate simulation of the effects of muscle actions on the movement of the eye. Of particular importance to the study of Listing's Law are its ability to simulate synchronized muscle actions and its ability to capture the pulley and no–pulley models of the oculomotor plant described by Miller (1989). The model is formalized using the notation of the Geometric Algebra (Hestenes, 1986).

The relationship between muscle lengths and eye attitudes depends on the geometry of muscle origins, insertions, and extraorbital, pulley–like constraints. The pulley, no–pulley, and all cases lying between these extremes can be constructed by defining a scalar function, $\zeta(t) \subseteq [0, 1]$, that determines the degree to which each model holds, viz:

$$\dot{\Theta} = [\zeta(\dot{\alpha}\hat{P} + \dot{\beta}\hat{Q} + \dot{\gamma}\hat{R}) + (1 - \zeta)(\dot{\mu}\Theta(x_i) \wedge x_\iota + \dot{\nu}\Theta(y_i) \wedge y_\iota + \dot{\xi}\Theta(z_i) \wedge z_\iota), \Theta]. \tag{9}$$

$\hat{P}$, $\hat{Q}$, and $\hat{R}$ are unit bivectors (or quaternions) that define the head–fixed rotation axes of the three muscle pairs in the no–pulley case. x_ι, y_ι, and z_ι are vectors that define head fixed points of tangency and x_i, y_i, and z_i are vectors that define eye fixed insertion points. These vectors are used to compute the current eye–fixed bivector for each muscle pair in the pulley case. $\Theta_s(g)$ is a spinor[2] that defines a saccadic rotation of the eye. The pulley model

[2]A spinor is a quaternion that represents a rotation.

holds exclusively when $\zeta = 0$ and the no–pulley model holds exclusively when $\zeta = 1$. In general, ζ can be a function of $\Theta, t, \dot{\alpha}, \dot{\beta}, \dot{\gamma}, \dot{\mu}, \dot{\nu}$, and/or $\dot{\xi}$. If $\dot{\alpha}$, $\dot{\beta}$, $\dot{\gamma}$, $\dot{\mu}$, $\dot{\nu}$, and $\dot{\xi}$ represent true rates of change of muscle lengths then, of necessity, $\dot{\alpha} = \dot{\mu}, \dot{\beta} = \dot{\nu}$, and $\dot{\gamma} = \dot{\xi}$.

Details of the simulation. The values of origin, tangent, and insertion points of the muscles were chosen so that rotations about each of the muscle planes formed by these points moved the gaze direction as specified in Figure 0.2. The tangent points were chosen to be $x_t = \{0, 0, 1\}$, $y_t = \{0, 1, 0\}$, and $z_t = \{0, 1, 0\}$. The initial positions of the insertion points were computed as follows. The initial x_i was set equal to $\sigma_1 = \{1, 0, 0\}$ and then rotated about the $\sigma_2 = \{0, 1, 0\}$ axis by $-25°$. The initial y_i and z_i were first set equal to $\sigma_1 = \{1, 0, 0\}$ and then rotated about the $\sigma_3 = \{0, 0, 1\}$ axis by $25°$. The initial y_i was then rotated about the σ_2 axis by $-10°$ and the initial z_i was then rotated about the σ_2 axis by $20°$. The head fixed axes were computed by

$$\hat{P} = (x_i \wedge x_t), \tag{10}$$

$$\hat{Q} = (y_i \wedge y_t), \tag{11}$$

and

$$\hat{R} = (z_i \wedge z_t). \tag{12}$$

During the course of the integration the spinor that has been computed thus far is used to move the muscle insertion points. The new muscle planes and muscle axes are then computed for the next increment in the saccade spinor. The LSODA numerical integration package (Petzold and Hindmarsh, 1987) provided accurate numerical integration. Each saccade was integrated from $t = 0$ to $t = 3.0$ with output from the integration taken at every $t_{out} = 0.05$ time units. Both the pulley and no–pulley models were simulated with similar results. The muscle insertion points were moved and the new axes of rotation were computed at every t_{out}. In the model, the size of rotations is controlled by the size of changes in tonic cell activities which in turn are controlled by the spatial gradient gains G_{lm} and G_{si}. The new eye attitude or gaze direction is used together with the spatial target vector to compute the new retinotopic target position via spherical trigonometry. At the end of a saccade a second light position, (x_2, y_2), is calculated. If the saccade is judged not to have been successful in foveating the target, a corrective saccade may be initiated by treating the second light as a first light. This judgement may be made in two ways: (1) determining whether both x_2 and y_2 are each below some threshold or (2) determining whether the projection of the gaze direction, g, onto the spatial target vector, t, i.e. $g \cdot t$, is above some threshold. The latter may be preferable because it measures accuracy equally in all retinotopic directions: It implies a circular fovea rather than a square one. The latter measure is used here.

Neural integration of spatial velocity commands can be problematic, as noted by Tweed, Misslisch and Fetter (1994). However, the step change in tonic cell activity and the subsequent integration performed on the muscle activities represent changes that occur in motor

coordinates, not spatial coordinates. The simultaneous action of muscle synergists means that the oculomotor plant acts, on average, more like a commutative plant. This is demonstrated by the following simulation results.

4 Analysis of Simulation Results

Typical simulation results are shown in Figure 0.4 as plots of saccade spinors expressed relative to the gaze direction as described by Tweed and Vilis (1990b). That is, in each trial of the simulation the model executes a number of saccades from various eye attitudes to random spatial target positions. The eye position quaternion (EPQ) that transforms the reference position into a given eye attitude is computed. The saccade spinors computed during the numerical integration of Equation 0.9 are not used. Instead, the matrix of direction cosines that rotates the reference attitude to a given gaze attitude is computed as described in Hestenes (1994). The eye position quaternion is then computed from this matrix as described by Tweed and Vilis (1990b). Though more efficient methods for recovering Q exist, this method was used in order to be most consistent with the quantitative methods used by experimentalists to characterize saccades (e.g. Tweed and Vilis, 1990b).

If, when plotted, the last three components of all the eye position quaternions form a plane, then Listing's Law holds. Recall, that the q_t component specifies a rotation about a head–fixed reference eye position. Note that the saccades were not all actually made from the reference position, they are merely being expressed as if they were. The other components, q_h and q_v, specify rotations about axes orthogonal to the reference position. If $q_t = 0$ everywhere, then the reference position is the primary position. This would be easily seen, since, in this case, all points would lie on the q_t axis when they were plotted against q_v or q_h. The plane would be tilted relative to the q_t axis when the reference position and primary position did not match exactly.

The parameters for the simulations were as follows: the horizontal and vertical ranges for the random targets were both 70°; $A = 100$, $G_{lm} = 0.001$ and $G_{si} = 0.0005$; the eye was reset to the initial position every 5 trials or if foveation was not achieved on a given trial within the allowed number of attempts; 3 attempts per trial were allowed; and 1000 trials were performed. This reset may correspond to a further assumption of a 'neutral' or 'at rest' position for the eye. Figure 0.4 shows that eye attitudes assumed after foveating saccades exhibit regularity that looks planar, but has some variance. Statistics shown below demonstrate that these attitudes do tend to obey Listing's Law. For simulations that generated the data plotted in Figure 0.4, a target was judged to be foveated when $gaze \cdot target \geq 0.99997$. This accuracy corresponds to a foveation acceptance zone that is 0.888° in diameter.

The simulations revealed that eye attitudes assumed, both when the target is foveated and when it is not, tend to obey Listing's Law more closely as the accuracy criterion is increased, as shown in Figure 0.5. This is true for both the pulley and no–pulley models.Adherence to the law was measured by the standard deviation, σ^2, of the torsional component from the line of best fit between the torsional, q_t, and horizontal, q_h, components of the eye

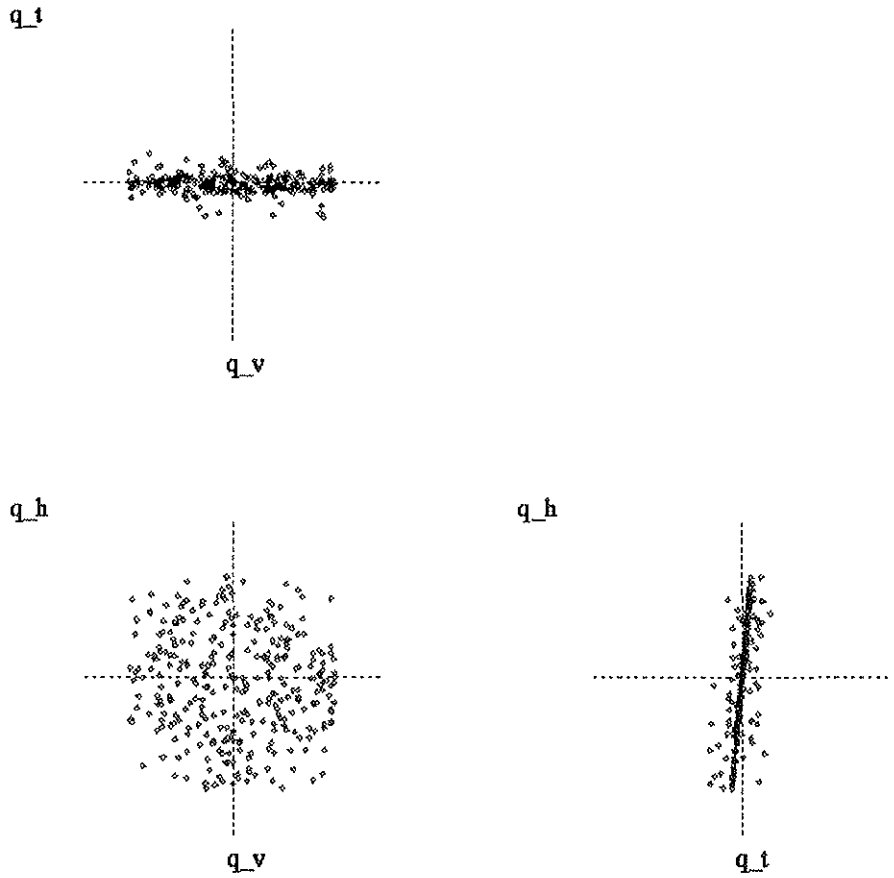

Figure 4: Eye attitudes assumed upon accurate fovcation do obey Listing's Law. Fovcation was achieved in 316 of 1000 trials. 3 attempts per trial were allowed. Fovcation was deemed to be accurate when $gaze \cdot target \geq 0.99997$. This corresponds to a foveal diameter of less than a degree.

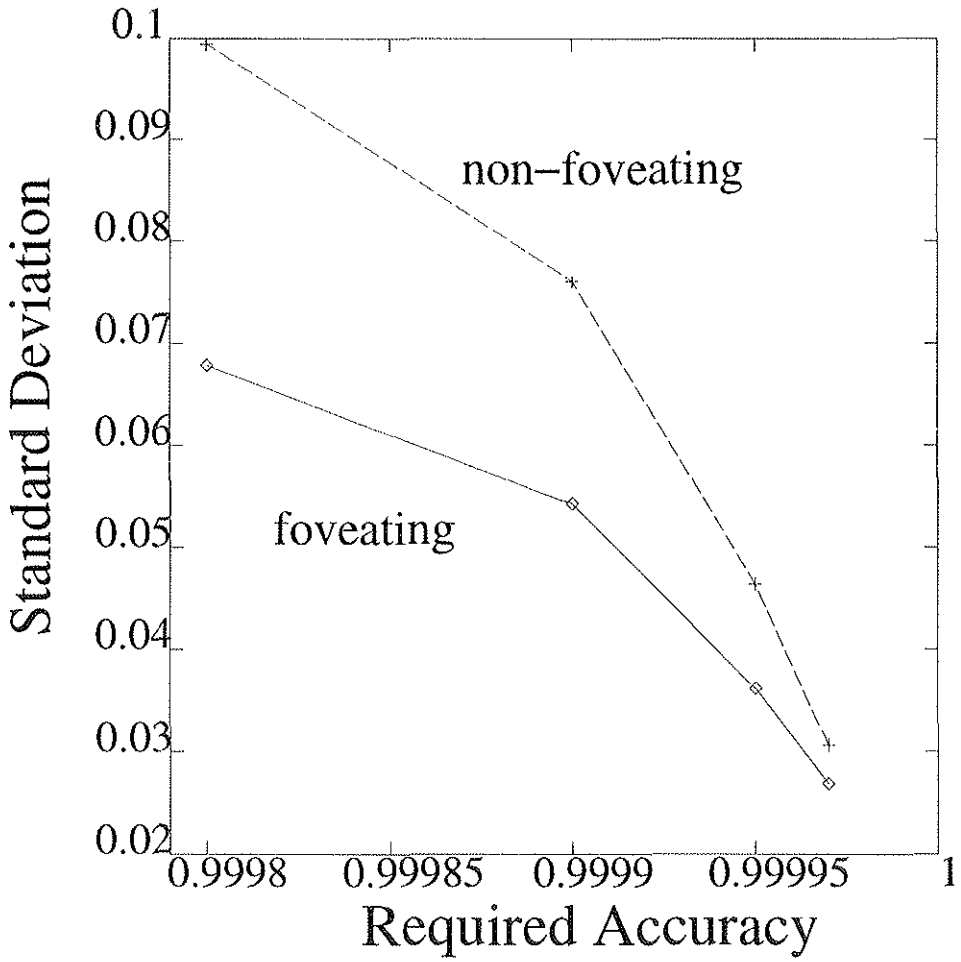

Figure 5: Adherence to Listing's Law increases as required accuracy increases for eye attitudes assumed after both foveating and non-foveating saccades. Plotted are the standard deviations, σ^2, of the torsional component of the eye position quaternions as a function of required saccade accuracy. Both foveating and non–foveating saccades converge, though the attitudes assumed after non–foveating saccades do slightly less well.

position quaternions. Accuracy was specified by the minimum dot product of the gaze and target positions. It may seem surprising that the adherence of eye attitudes for non–foveated targets increases along with those for foveated targets. This occurs because as the accuracy requirement increases, more quite–accurate saccades fall below the criterion, and therefore into the non–foveating saccade category. This raises the mean accuracy of the non–foveating category, and therefore reduces the deviation from Listing's Law.

These standard deviations may be translated into maximum degrees of rotation about the primary position by

$$\sigma^2 = sin(\phi/2) \tag{13}$$

and

$$\phi = sin^{-1}(\sigma^2)/2 \tag{14}$$

So by the empirical rule (of statistics) for 0.99997, 68% of attitudes for foveated targets require less than $1 \times \phi = 0.77$ degrees of rotation about the primary position and 95% have less than $2 \times \phi$ degrees of rotation. This is close to the variability observed by Ferman et al (1987) and it suggests another source of variability. This source is the foveation accuracy that the oculomotor system maintains.

5 Conclusion

The model presented predicts that naive saccadic control systems, such as might be found in an infant, already exhibit behavior that closely approximates Listing's Law. This result suggests that a high internal criterion of accuracy for saccades made reactively with this model can generate a stable set of terminal muscle coordinates suitable for learning accurate single–step saccades that are even more obedient to Listing's Law. That is, accuracy helps translate the innate spatial gradient into a statistically stable and Listing's Law obedient baseline for learning accurate foveation. An adaptive saccadic control system with foveation gated learning has been shown to generate single–step saccades that obey Listing's Law (Pribe, 1994).

It remains to explore behavior that may emerge from the interaction of the control system with the dynamics of the physical plant. This would include effects such as the small transient deviations in torsional eye position during saccades, called "blips", reported by Tweed, Misslisch, and Fetter (1994). A physiologically plausible exploration of these effects would require the expansion of the biomechanical model used here, which is a kinematic model, to include dynamic effects such as viscosity and inertia. It would also require a saccade generator model, such as that of Grossberg and Kuperstein (1986) or Scudder (1988), that includes the activation 'pulse' used *in vivo* to overcome inertia.

In the theory presented here, Listing's Law is thought to reflect an uneven sampling of biomechanically possible 3–D spatial attitudes due to two properties of the oculomotor system. The first property is the reduced representation necessitated by the fact that components of the sensory apparatus, such as the retina and the superior colliculus, have a 2–D

topology, whereas the motor system is controlling a plant with 3 rotational degrees of freedom. The second property is the synchronization of synergists: For a given movement all the muscles begin to move, move, and stop moving simultaneously. This reduces the space of possible single–step eye movements and biases the sampling of eye attitudes by a naive oculomotor control system.

APPENDIX

The Time Derivative of the Gaze Attitude

Using the notation of Hestenes (1986), define a saccadic rotation of the eye, $\Theta_s(g)$, as the application of a quaternion or spinor, S, to the eye or gaze attitude, g:

$$\Theta_s(g) = SgS^{-1} \tag{15}$$

The time derivative of the gaze attitude, $\dot{\Theta}(g)$, depends upon a change in the saccade spinor:

$$\dot{\Theta}(g) = \dot{S}gS^{-1} - SgS^{-1}\dot{S}S^{-1} \tag{16}$$

This can be reduced to

$$\dot{\Theta} = [\dot{S}S^{-1}, \Theta_s] \tag{17}$$

where $[A, B]$ is the commutator, $AB - BA$, of A and B (Pribe and Cohen, 1995, and Pribe, 1994).

References

Ferman, L., Collewijn, H., and Van Den Berg, A. V., (1987), A direct test of Listing's Law – I. Human ocular torsion measured in static tertiary positions, *Vision Research*, v. 27, no. 6,

Grossberg, S., and Kuperstein, M. (1986). **Neural Dynamics of Adaptive Sensory-Motor Control**, Pergammon Press, NY, NY

Helmholtz, H. L. F. von (1867/1962). Movements of the Eyes, In **Helmholtz's Treatise on Physiological Optics**, translated from the third German edition, J. P. C. Southall, ed., vol. 3, Dover, NY NY,

Hepp, K., van Opstal, A. J., Straumann, D., Hess, B. J. M., and Henn, V., (1993). Monkey Superior Colliculus Represents Rapid Eye Movements in a Two–Dimensional Motor Map, *Journal of Neurophysiology*, **69**, no. 3

Hestenes, D. (1986). **New Foundations for Classical Mechanics**, D. Reidel, Boston

Hestenes, D. (1994). Invariant Body Kinematics: I. Saccadic and Compensatory Eye Movements, *Neural Networks*, **7:1**, 65–77

Kandel, E. R., and Schwartz, J. H. (1985). **Principles of Neural Science**, Second Edition, Elsevier, NY NY

Miller, J. M. (1989), Functional Anatomy of the Normal Human Rectus Muscles, *Vision Research*, **29:2**, 223-240

Petzold, L.R. and Hindmarsh, H. (1987). LSODA Numerical Integration Package. *Technical Report*, Lawrence Livermore National Laboratory, Livermore, California.

Pribe, C. A. (1994). **Neural Dynamics of Gaze and Gait: Spatial Sensory–Motor Control and Temporal Pattern Generation**, *Doctoral Dissertation*, Boston University ,UMI Order #9402003

Pribe, C. A., and Cohen, M. A., (1995) A Biomechanical Model of Human Oculomotor Plant Kinematics Based Upon Geometric Algebra, *Neural Networks*, In Press

Scudder, C. (1988). A new local feedback model of the saccadic burst generator, *Journal of Neurophysiology*, **59**, 1455–1475

Tweed, D. B., and Vilis, T. (1990a), The Superior Colliculus and Spatiotemporal Translation in the Saccadic System, *Neural Networks*, **3**, 75-86

Tweed, D. B., and Vilis, T. (1990b), Computing Three–Dimensional Eye Position Quaternions and Eye Velocity from Search Coil Signals, *Vision Research*, **30**, no. 1, 97-110

Tweed, D. B., and Vilis, T. (1990c), Geometric Relations of Eye Position and Velocity Vectors during Saccades, *Vision Research*, **30**, no. 1, 111-127

Tweed, D. B., and Vilis, T. (1992a), Rotation of Listing's Plane During Vergence, *Vision Research*, **32**, no. 11, 2055-2064

Tweed, D. B., and Vilis, T. (1992b), Three–Dimensional Properties of Human Pursuit Eye Movements, *Vision Research*, **32**, no. 7, 1225–1238

Tweed, D., Misslisch, H., and M. Fetter, Testing Models of Oculomotor Velocity–to–Position Transformation, *Journal of Neurophysiology*, **72**, no. 3, 1425–1429